Vapor Sensor Realized in an Ultracompact Polarization Interferometer Built of a Freestanding Porous-Silicon Form Birefringent Film

Beom-hoan O, Rong Liu, Yang Yang Li, Michael J. Sailor, and Yeshaiahu Fainman, *Senior Member, IEEE*

***Abstract*—A novel vapor sensor that uses polarization interferometry in a form birefringent porous-silicon film is introduced, analyzed, and experimentally characterized. Simulations and analysis of accuracy, versatility, stability, and control of dynamic range of the device are provided. The simulation accurately predicts the polarization interference signal, which is used to estimate the effective refractive indexes characterizing the form birefringence of a porous-silicon film with 0.001 accuracy. The device was tested for the detection of heptane concentration in a range of 342–20 000 ppm (=2.0%).**

***Index Terms*—Form birefringence, polarization interferometry, porous silicon, vapor sensor.**

I. Introduction

IMMENSE EFFORTS have been made recently in developing optical devices made of porous silicon [1] utilizing well-established microfabrication techniques. Having many advantages, such as large interaction surface area for sensing, simplicity and repeatability of fabrication, and compatibility with other well-established silicon technologies, porous silicon has attracted much attention in the field of sensor technology. For hazardous environment applications, such as sensing flammable vapors and gases, optical sensors attracted appreciable attention in contrast to well-established electronic methods based on capacitance [2] and conductivity [3] measurements. There exist several different methods of optical sensing based on optical reflectivity [4], [5], birefringence [6], [7], and using properties of optical waveguides [8]. However, their practical implementations are somewhat complicated, and the characterization shows some discrepancies between calculations and measurements [4]–[8].

In this manuscript, we report a novel realization of a vapor sensor using a free-standing porous-silicon film. The method employs a form birefringence effect in porous-silicon film to construct an ultracompact polarization interferometer. The sensitivity of the device is achieved via the dramatically enhanced interaction area of the porous silicon combined with high sensitivity phase measurement via the analysis of the polarization interference signal.

Manuscript received December 12, 2002; revised February 26, 2003. This work was supported by the National Science Foundation, ONR, and DARPA/SPAWAR, by the Ministry of Education through the BK21 Project, and in part by the Korea Science and Engineering Foundation under Grant 01-1999-000-00225-0.

B. O is with the Semiconductor Division, School of Electrical and Computer Engineering, INHA University, Inchon 402-751, Korea (e-mail: obh@inha.ac.kr).

R. Liu and Y. Fainman are with the Department of Electrical and Computer Engineering, University of California, San Diego, La Jolla, CA 92093 USA.

Y. Y. Li and M. J. Sailor are with the Department of Chemistry and Biochemistry, University of California, San Diego, La Jolla, CA 92093 USA.

Digital Object Identifier 10.1109/LPT.2003.811344

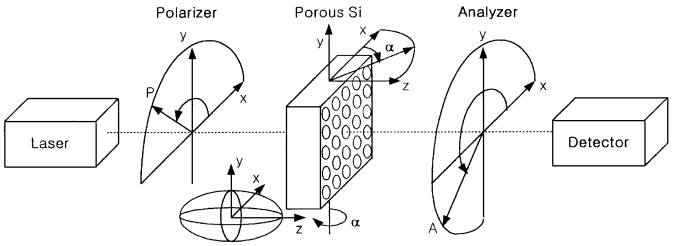

Fig. 1. Schematic of experimental setup and the index ellipsoid of a porous-silicon film.

II. Experimental Setup and Polarization Interferometry With Porous-Silicon Film

Porous-silicon films are fabricated in a heavily doped p-type <100> silicon wafer by anodic etching in aqueous high-frequency (49 wt%) solution with ethanol in the volume ratio of 3 : 1 at room temperature [9]. Atomic-force microscopy was used to determine the average pore size of less than 20 nm in diameter, whereas the porosity of 82% was estimated using the gravimetric method. The diameter of a fabricated porous-silicon film is about 10–13 mm. As the micro-pores are distributed uniformly with their axis perpendicular to the surface of silicon wafer [10], the resulting artificial form birefringent porous-silicon film can be considered to be a positive uniaxial anisotropic material due to the in-plane rotational symmetry, resulting in optic axis collinear with the direction of the pores. Consequently, the effective dielectric constant for the optical field polarized in the plane of incidence (i.e., transverse magnetic (TM) or extraordinary polarization) will depend strongly on the angle of incidence (see Fig. 1), whereas the effective dielectric constant for the optical field polarized perpendicular to the plane of incidence (i.e., transverse electric (TE) or ordinary polarization) will remain constant. The strong polarization dispersion in a porous-silicon film can be used to construct an ultracompact, high sensitivity porous-silicon polarization interferometer with a special emphasis on sensors applications.

A schematic diagram of our experimental setup is shown in Fig. 1. For our experiments, we use an external-cavity tunable diode laser operating at a wavelength of 1.52 μm to minimize the absorption losses upon propagation through silicon (i.e.,

photon energy below silicon band edge). The laser beam is first introduced into a polarizer and then used to illuminate the porous-silicon sample. The transmitted light is then analyzed by a polarization analyzer and introduced into a photodetector for measurements. The porous-silicon sample is mounted on a precision rotation stage, allowing precise control of the surface normal orientation. Initially, we align the propagation direction of the optical beam to be collinear with the axis of the pores, i.e., the optic axis, setting $\alpha = 0$. For sensing experiments, we insert the porous-silicon sample into a custom-made glass flow cell connected to a bubbler for the exposure to solvent vapors in a controlled and reproducible manner.

The polarizer and analyzer are aligned perpendicular with respect to each other and at 45° with x-axis in the x–y plane. Under simplifying assumptions of minimal absorption and surface reflections in this setup, we find the transmitted intensity at the output of the analyzer

$$I(\alpha) = \frac{1}{2}\left[a^2 + b^2 - 2ab\cos(\Delta\phi(\alpha))\right] \tag{1}$$

$$\Delta\phi(\alpha) = \frac{2\pi}{\lambda}\left[n_e(\alpha)L_e(\alpha) - n_o(\alpha)L_o(\alpha)\right] \tag{2}$$

where a and b are the amplitudes of transmitted electric fields for TE and TM polarizations, respectively, $\Delta\phi(\alpha)$ is effective phase difference for ordinary and extraordinary polarized components, and λ, $n_{e(o)}(\alpha)$, and $L_{e(o)}(\alpha)$ are the laser wavelength in vacuum, angle-dependent effective refractive indexes, and the geometric path lengths in a film for extraordinary (ordinary) component for given angle, respectively. Note that $n_o(\alpha) = n_o$ (ordinary index) and $n_e(\alpha)$ is a function of three parameters, α, n_o, and n_e (extraordinary index) in an index ellipsoid. Notice that the effective phase difference, $\Delta\phi(\alpha)$, does not depend linearly on the angle of incidence α, giving rise to a chirp-like behavior. The interference signal has chirp-like harmonic dependence on α, which is important for accurate analysis and better understanding its functional dependence using numeric simulation.

III. Experimental Data and Analysis

The polarization interference signals are obtained by measuring the transmitted optical intensity for each porous-silicon film. Fig. 2(a)–(d) shows the comparison of measured and simulated polarization interference signals versus the angle of incidence for several samples of porous-silicon form birefringent films with thicknesses of 72, 100, 198, and 228 μm, respectively.

From Fig. 2, we observe a chirp-like harmonic behavior with increasing chirp as the thickness of the form birefringent film increases at all angles of incidence. As the angle of incidence increases, the interval of the oscillatory signal increases (see Fig. 2). This peculiar uneven sinusoidal variation helps the data fit process to extract reliable and accurate values of optical indexes, and improves the fit accuracy of all extremums. After obtaining a curve fit, any slight variation of the indexes, even on the order of ~0.001, deteriorates the accuracy of the fit significantly, causing some of the peaks to shift by about ~0.3°. On the other hand, if both index values n_e and n_o are varied simultaneously, the error range increases [see also expression for $\Delta\phi(\alpha)$ in (2)]. The index pair values of best fit and the corresponding error ranges for all cases of transmitted intensity curves in Fig. 2 are summarized for comparison in Table I.

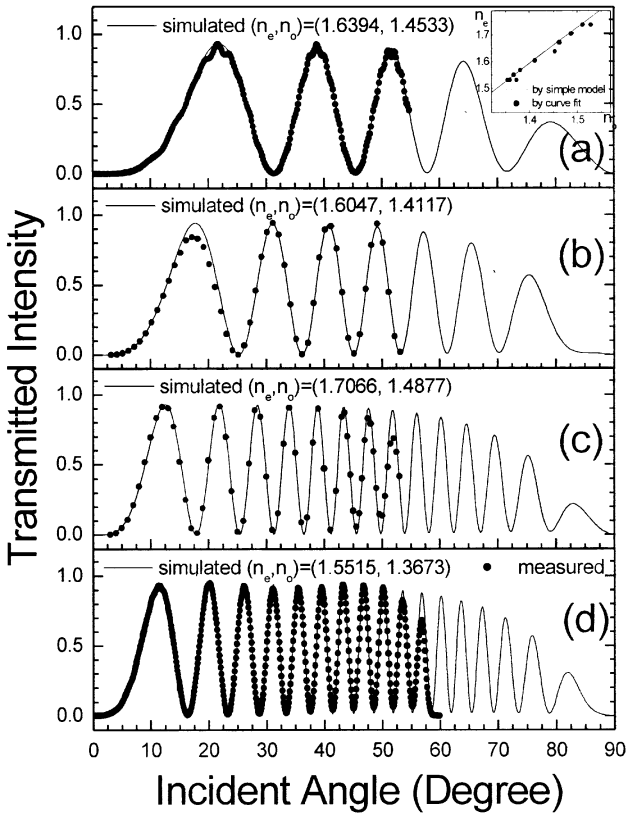

Fig. 2. Polarization interference signals versus angle of incidence for porous-silicon film samples with thickness of (a) 72, (b) 100, (c) 198, and (d) 228 μm. Inset figure denotes all index pair coordinates in Table I. The simple model agrees with the variations of all the index pair value quite well.

TABLE I
Comparison of Optical Index Pairs and Error Ranges of Four Different Porous Silicon Samples, of Which Porosity is About 82%, Estimated by Gravimetric Method

Porous Si sample	$(n_e, n_o)_{lower}$	$(n_e, n_o)_{best}$	$(n_e, n_o)_{upper}$	$(\pm\delta n_e, \pm\delta n_o)$
72 μm	(1.5330, 1.3728)	(1.6394, 1.4533)	(1.7393, 1.5283)	(±0.10, ±0.08)
100 μm	(1.5330, 1.3590)	(1.6047, 1.4117)	(1.6733, 1.4618)	(±0.05, ±0.05)
198 μm	(1.6733, 1.4635)	(1.7066, 1.4877)	(1.7393, 1.5117)	(±0.033, ±0.024)
228 μm	(1.5330, 1.3541)	(1.5515, 1.3673)	(1.5692, 1.3803)	(±0.018, ±0.013)

Note that the error range decreases as the thickness increases. This occurs due to the increase of phase lag, leading to more oscillation periods (zero-crossings), thereby improving the accuracy of the fit. It is interesting that the coordinates of all index pairs in Table I are plotted quite closely to a simple model line in an index plane (n_e, n_o), as shown in the inset figure of Fig. 2. Although detailed discussion on this model is beyond the main objective of this letter, this simple parametric relation for form-birefringent dielectrics can be derived from a model of a simple rectangular cylinder shape pore structure with a parametric variable related to porosity. The coincidence between the estimated index pair values and a simple birefringent model is also a good evidence to support the quality and reliability of the simulated curve fit procedures and results.

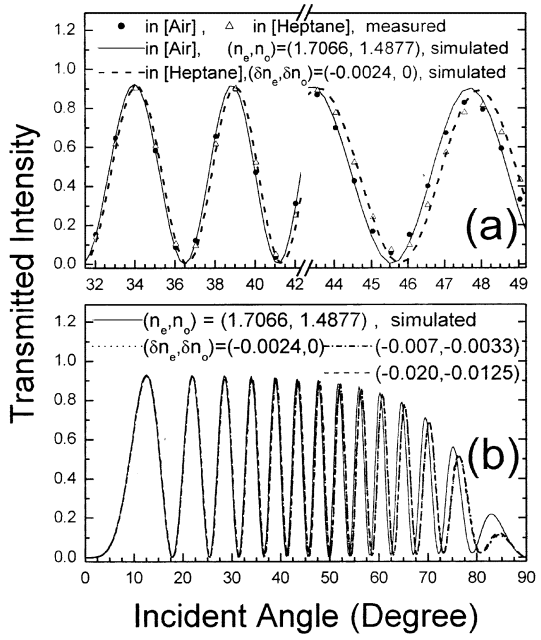

Fig. 3. Comparison of the polarization interference signal versus angle of incidence for a porous-silicon sample of thickness 198 μm in air and in vapor of heptane with concentration of 2.0%. (a) Enlarged view near middle peaks for details. (b) Whole range view for the comparison of pair variations. Note the peak shifts are not linear.

Next, we discuss the effects in porous-silicon polarization interferometer that lead to its application for chemical sensing. When the porous-silicon film sample is exposed to solvent vapors, effective indexes n_o and n_e slightly changed due to the variation of surface states originated from the difference in electron affinities between silicon and the vapor molecules adsorbed on the surface boundary of all pores. The local variation of index on the surface boundary, even though quite small, causes shifts in the polarization interference signal with chirp-like harmonic behavior, and thus, it provides quite large change in the output intensity when set at a high sensitivity bias angle of incidence. For experiments on the vapor sensing of heptane vapor of 2.0% concentration, the change of the polarization interference signal is shown in Fig. 3 for a film of thickness 198 μm. The enlarged curve view is shown in Fig. 3(a) near middle peaks for details, and the whole range view is shown in Fig. 3(b) for the comparison of curves with various pair variations. Note that the shift of peaks is not linear in α, although it is not so clear in this whole view.

For this experiment, we used same sample as for Fig. 2(c). The pattern for "in heptane" was obtained by a small adjustment of δn_e, as shown in Fig. 3(a), or (δn_e, δn_o), as shown in Fig. 3(a), in the simulations. The simulated curves in entire region, as shown in Fig. 3(b), enable us to design an appropriate α for desired sensitivity by revealing all nonlinear shifts in a changed pattern. Note that if the pair variation exceeds (δn_e, δn_o) = (-0.02, -0.0125), the fit deviates significantly from the measured one, while three curves of careful pair variations within error range look similar. The patterns for the concentration of heptane from 342 to 20 000 ppm (=2.0%) are fitted well by a linear variation of δn_e. Furthermore, a porous-silicon film shows quite stable behavior for repeated experiments.

IV. Conclusion

A novel vapor sensor using a freestanding porous-silicon form birefringent film is realized experimentally, and the characteristics are analyzed using computer simulations. It enables us not only to design an appropriate dynamic range and sensitivity by optimizing the angle of incidence α, but also to extract accurate index values of birefringence within small error of just $\sim$0.001 for index variation. Even without any careful optimization, the concentration of heptane vapor from 342 to 20 000 ppm (=2.0%) can be detected experimentally with high reproducibility. A freestanding porous-silicon form birefringent film provides a basis for the construction of ultracompact polarization interferometer when sandwiched between a polarizer–analyzer pair, enabling fast and versatile sensing mechanism with not only the accuracy from the high sensitivity of interferometry but also the convenience from the simplicity of implementation for the detection of vapors or gases, especially in a hazardous environment.

References

[1] A. G. Cullis, L. T. Canham, and P. D. J. Calcott, "The structural luminescence properties of porous silicon," *J. Appl. Phys.*, vol. 82, no. 3, pp. 909–965, 1997.

[2] A. Motohashi, M. Kawakami, H. Aoyagi, A. Kinoshita, and A. Satou, "Gas identification by a single gas sensor using porous silicon as sensitive material," *Jpn. J. Appl. Phys.*, vol. 34, pp. 5840–5843, 1995.

[3] R. Angeluccia, A. Poggia, L. Doria, G. C. Cardinalia, A. Parisinia, A. Tagliania, M. Mariasaldia, and F. Cavanib, "Permeated porous silicon for hydrocarbon sensor fabrication," *Sens. Actuators A*, vol. 74, pp. 95–99, 1999.

[4] J. Gao, T. Gao, and M. J. Sailor, "Porous silicon vapor sensor based on laser interferometry," *Appl. Phys. Lett.*, vol. 77, pp. 901–903, 2000.

[5] P. A. Snow, E. K. Squire, and P. St. J. Russell, "Vapor sensing using the optical properties of porous silicon Bragg mirrors," *J. Appl. Phys.*, vol. 86, pp. 1781–1784, 1999.

[6] E. Gross, D. Kovalev, N. Kunzner, V. Yu. Timoshenko, J. Diener, and F. Koch, "Highly sensitive recognition element based on birefringent porous silicon layers," *J. Appl. Phys.*, vol. 90, pp. 3529–3532, 2001.

[7] M. E. Kompan, J. Salonen, and I. Yu. Shabanov, "Anomalous birefringence of light in free-standing samples of porous silicon," *J. Exp. Theor. Phys.*, vol. 90, pp. 324–329, 2000.

[8] H. F. Arrand, T. M. Benson, A. Loni, R. Arens-Fischer, M. Kruger, M. Thonissen, H. Juth, and S. Kershaw, "Novel liquid sensor based on porous silicon optical waveguides," *IEEE Photon. Technol. Lett.*, vol. 10, pp. 1467–1469, Oct. 1998.

[9] R. Liu, T. A. Schmedake, Y. Y. Li, M. J. Sailor, and Y. Fainman, "Novel porous silicon vapor sensor based on polarization interferometry," *Sens. Actuators B*, vol. 87, pp. 58–62, 2002.

[10] S. Zangooie, R. Jansson, and H. Arwin, "Investigation of optical anisotropy of refractive-index-profiled porous silicon employing generalized ellipsometry," *J. Mater. Res.*, vol. 14, pp. 4167–4175, 1999.